

Forces on Submerged Cylinders Oscillating near a Free Surface

Jin S. Chung*

Lockheed Missiles and Space Company, Inc., Sunnyvale, Calif.

Forces on submerged, two-dimensional bodies of constant circular or square cross section oscillating in water of infinite depth have been measured using a forced oscillation test. The bodies were forced to sway and heave sinusoidally with small amplitudes, for several submergences below a free surface. The added-mass and wave-damping coefficients are shown to be influenced strongly by the free-surface effect and are presented as a function of frequency and direction of oscillation and of depth of submergence from the free surface. There appears to be a critical frequency that was measured consistently for heave oscillations near the free surface and was not predicted by existing theories. The measured coefficient values for the sway and heave oscillations of the circular cross section near the free surface were shifted in frequency, whereas the corresponding theoretical coefficients are identical. Comparisons of the experimental results with computations by a potential theory show reasonably good agreement. Use of the coefficients in equations of motion for floating ocean structures is described.

Nomenclature

a	= radius of circular cross section or half-beam
a_{yy}	= sway added-mass coefficients ($a_{yy} = Y_i/m\omega^2\eta - m'/m$)
a_{zz}	= heave added-mass coefficients ($a_{zz} = Z_i/m\omega^2\zeta - m'/m$)
b_{yy}	= sway wave-damping coefficients ($b_{yy} = Y_0/m\omega\eta - b_{yy}^*/m$)
b_{zz}	= heave wave-damping coefficients ($b_{zz} = Z_0/m\omega\zeta - b_{zz}^*/m$)
b_{yy}^*	= sway damping coefficients obtained at $\bar{s} = 8(b_{yy}^* = Y_0/\omega\eta)$
b_{zz}^*	= heave damping coefficients obtained at $\bar{s} = 8(b_{zz}^* = Z_0/\omega\zeta)$
g	= gravitational acceleration
h	= water depth
\bar{h}	= nondimensional water depth ($\bar{h} = h/a$)
L	= total length of cylinder models
m	= displaced-water mass ($m = \rho\pi a^2\ell$)
m'	= tare mass of test section obtained in air test
s	= submerged distance of cylinder axis below still-water surface
\bar{s}	= nondimensional submergence ($\bar{s} = s/a$)
Y_i, Z_i	= sway and heave amplitudes, respectively, of in-phase force
Y_0, Z_0	= sway and heave amplitudes, respectively, of out-of-phase (or quadrature) force
ρ	= mass density of water
ω	= oscillation frequency of cylinder models
$\bar{\omega}$	= nondimensional oscillation frequency ($\bar{\omega} = \omega a^2/g$)
ℓ	= test-section length of cylinder models
η	= amplitude of sway oscillation
ζ	= amplitude of heave oscillation

I. Introduction

DETERMINATION of the hydrodynamic force acting on the submerged members of floating ocean structures forms a linear boundary-value problem in potential theory. The superposition principle holds, and the actual phenomenon then consists of the sum of two parts: 1) harmonic oscillations of the submerged member in still water,

and 2) waves exerting on the restrained structural members. The two fields can be investigated separately. This paper experimentally investigates the hydrodynamic coefficients of the harmonic oscillations of the submerged member in still water having a free surface. The hydrodynamic coefficients of two-dimensional submerged bodies influenced by the free-surface effect as calculated using potential theories (by Yamamoto¹ for a circular cross section and Frank² for an arbitrary cross section) have not been validated with experimental data.^{3,4} For many practical applications, the matter may be solved by combining elementary two-dimensional solutions for the hydrodynamic forces in a strip theory. Members of many floating ocean structures can be approximated³ as two-dimensional except for those parts close to joints between members. Strip-theory computations of motions of the floating ocean structures, which ignore the flow interferences at joints or between members along with possible end effects, appear to be reasonably accurate for practical applications.³

Most floating ocean structures for offshore petroleum drilling and production operations consist of members of circular and other cross sections with their submerged members frequently close to the free surface. It is well known that, for submerged bodies oscillating in an infinite fluid,⁵ the added-mass coefficients are constants, and the wave damping is zero. But as the submerged body oscillates close to the free surface, the free-surface effect can influence the added-mass and wave-damping coefficient values greatly as a function of the frequency and direction of oscillations. Although it is not expected for a circular-cross-section model oscillating very close to the free surface, the theories in Refs. 1 and 2 predict that the added-mass and wave-damping coefficients of the circular cross section are identical for sway and heave oscillations.

These frequency-dependent coefficient values provide better accuracy for computing motion of the structure and forces on the submerged members. Many previous computations of motions and forces for floating structures (see a survey in Refs. 3 and 4) have used the constant values of added-mass coefficients and zero wave damping obtained for an infinite fluid. A few other computations of motion³ used theoretical coefficients,² which considered the free-surface effect and which improved the accuracy of the motion computations.

As a contribution to this matter, with emphasis on practical applications, a series of experiments was carried out to determine the two-dimensional added-mass and wave-damping coefficients, including the free-surface effect, in

Received Nov. 23, 1976.

Index categories: Hydrodynamics; Marine Hydrodynamics, Vessel and Control Surface; Marine Vessel Design (including Loads).

*Research Specialist, Hydrodynamics Department, Research and Development Division, Member AIAA.

order to check validity of the predictions by the potential theory.² In-phase and quadrature forces linear with the oscillation amplitude were measured by the planar-motion mechanism.⁶ Two submerged, horizontal, two-dimensional models having circular or square cross section were forced to oscillate sinusoidally in sway and heave at several submergences near a free surface. The limiting range of the free-surface effect on the coefficients is discussed, together with the practical aspects of the use of the measured data. Theoretically² computed coefficients are compared with the experimental data. The measured added-mass coefficients are presented in a form suitable, within the range of the experimental variables, with the force equation.^{3,7} Force components that can be caused by the effects of viscosity, separation, and large-amplitude oscillation are not treated in this paper.

II. Potential Theory

The hydrodynamic problem arising from the harmonic motion of an infinitely long, submerged body oscillating near the free surface of an ideal fluid has been solved by Yamamoto¹ for a circular cross section and by Frank² for a body of arbitrary cross section with lateral symmetry. Coefficient values computed in Ref. 1 for a circular cross section agree well with the corresponding coefficients computed by the method in Ref. 2 only when the body is not too close to the free surface. The velocity potential must satisfy the following requirements in two dimensions: Laplace's equation, the linearized free-surface condition, and the radiation condition. In addition, every disturbance in the fluid must vanish at infinite depth, and the normal component of the fluid velocity on the body surface is equal to the same component of the body-surface velocity, both taken in the mean position of the cylinder. The underlying assumptions are that the fluid is inviscid and incompressible, the flow is irrotational, the fluid domain is infinitely large, the motion amplitude is small with respect to the dimensions of the cross sections, and the generated waves have amplitudes that are small with respect to the wavelength.

It is well known that these conditions are fulfilled approximately in many problems associated with floating-structure motions, so that the theoretical solution is of significant value both qualitatively and quantitatively. The results of the experiments will have to show to what extent they validate the theoretical computations. For the present investigation, Frank's method of computations, which can treat both circular and square cross sections, is used.

III. Experiments

General Setup

Experiments were conducted in a towing tank, of which dimensions are 122 m in length and 7.62 m in width. Water depth was $h=4.57$ m. About halfway its length was the

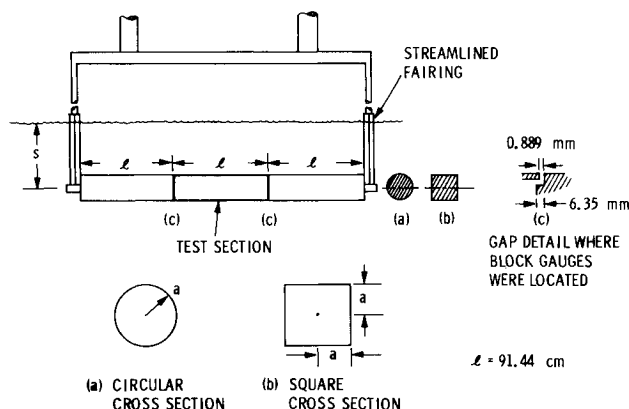


Fig. 1 Schematic of the two models of circular and square cross sections.

planar motion mechanism (PMM)⁶ installed on a stiff towing carriage, so that the axis of the horizontal model was perpendicular to the tank sidewalls. Braces were installed between the PMM assembly and the towing carriage for stiffness, and the entire carriage was lifted off its wheels and supported on blocks to provide a rigid base during testing. A sonic probe measured the outgoing waves at a distance of about 2 m from the axis of the model.

The forced harmonic oscillation experiments were conducted for two models of circular and square cross sections, the latter with sharp corners (Fig. 1). These two cylinder cross sections commonly have been used for submerged members of semisubmersible (floating) drilling structures.³ To minimize possible scale effects such as those associated with cross-flow drag at low Reynolds numbers, as well as measurement errors, the models were made as large as possible, yet compatible with the tank dimensions.

Force measurements were made by means of standard 10.16-cm modular force gages, which are described in Ref. 6. These gages are essentially flexure boxes machined out of a solid block of ARMCO 17-4 PH stainless steel. The deflection

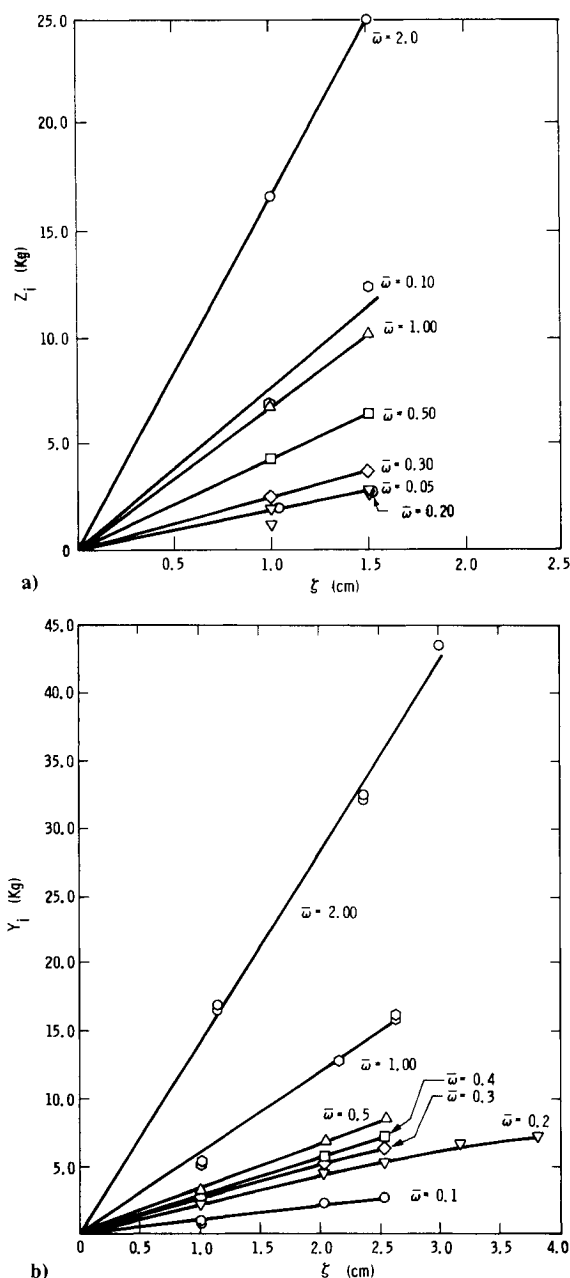


Fig. 2 Linearity of the in-phase force as a function of oscillation amplitudes of the circular-cross-section model; $\xi = 1.25$.

of the flexures is a linear function of applied force and is sensed by a variable reluctance gage. The force was shared by two gages, one on each side of the test section.

To provide accurate and continuous measurements of the oscillation amplitudes of the model, a cable-pulley-potentiometer arrangement was used. The electrical signal, which was calibrated as a function of amplitude, was recorded on an $X-Y$ plotter.

Two-Dimensionality

In order to assure that the two models of $2a = 22.86$ cm in diameter or beam would represent hydrodynamically two-dimensional sections, the test section of each model comprised only the middle third ($\ell = 91.44$ cm) of the $L = 274.5$ -cm models. The length-to-diameter ratio of each model was $L/2a = 12$. The only connections between the three segments were the two modular force gages just described, one at each connection. An average clearance of 0.089 cm was maintained between the surfaces of the segments, and throughflow at the connections was prevented by a labyrinth arrangement as shown in Fig. 1. The vertical rods were equipped with streamlined strut coverings to minimize possible surface disturbances during the sway oscillations, and supported each end of the model. To minimize cross-flow reflection at the tank sidewalls of waves generated by each end of the model, the tank-water level was raised so that the overhangs on the sidewalls served as wave absorbers.

As a further check on two-dimensionality, extension pieces of 60.96 cm in length were added to each end of the circular-cross-section model. Test results with and without these extension pieces agree very well with each other, confirming that the test section as designed and used for the series of experiments experienced little three-dimensional end effect. The experiments therefore proceeded without the extension pieces.

Measurements

The sway and heave oscillations were produced directly by the planar motion mechanism (PMM)⁶ with an adapter, which allowed either sway or heave. For heave oscillation, the amplitudes ζ of the PMM oscillator and of the models were identical. However, some bending of the rods supporting the model was recorded during the sway oscillations which increased slightly the model amplitudes η compared to the oscillator amplitudes. The deviations were less than 6 to 9% of the oscillator amplitudes for the square cross section and were less than 4 to 5% for the circular section at high frequencies ($1.0 \leq \bar{\omega} \leq 2.0$). The $\bar{\omega}$ is defined as $\bar{\omega} = \omega a^2 / g$, where g is the gravitational acceleration. In the low-frequency end ($\bar{\omega} \leq 0.5$), the deviations were less than 3%. The model amplitudes were used in reducing the force data to the coefficients.

Table 1 Principal characteristics of cylinders and oscillation amplitudes

	Cylinder cross sections	
	Circle	Square
Cylinder length L , cm	274.5	274.5
Test-section length ℓ , cm	91.44	91.44
Diameter or beam $2a$, cm	22.86	22.86
Oscillation amplitudes tested at each frequency and $\bar{s} = 1.25$		
Sway η , cm	1.016, 2.032, 2.540, 3.048, 3.810	1.016, 2.032, 2.720
Heave ζ , cm	1.016, 1.524	1.016, 2.032
Linear oscillation amplitudes used for the test series		
Sway η_{\max} , cm	2.540	2.032
Heave ζ_{\max} , cm	1.016	1.016

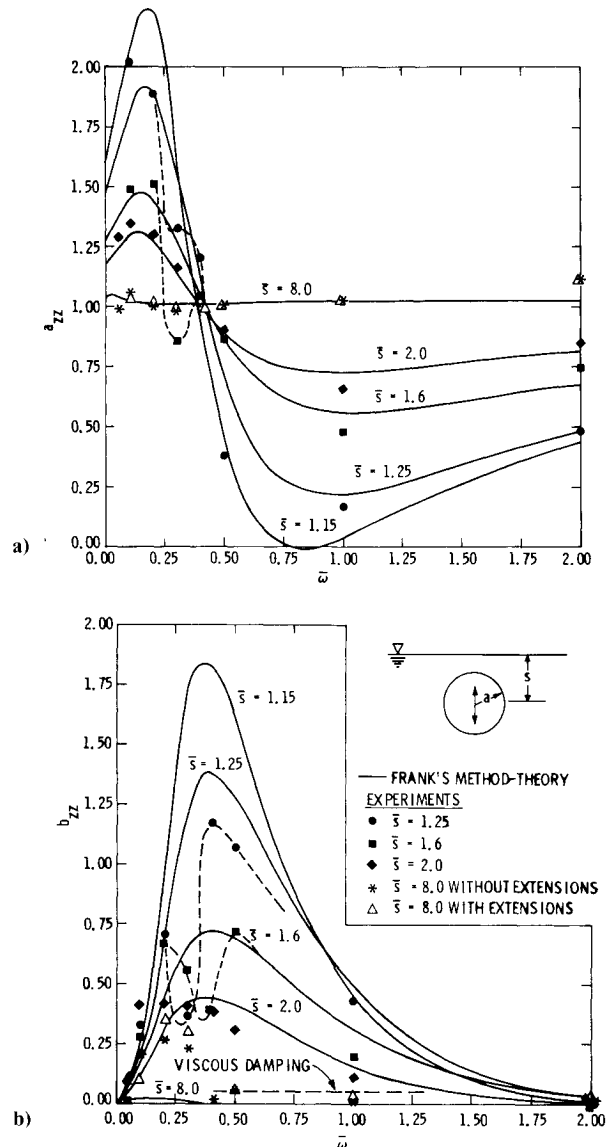


Fig. 3 a) Added-mass coefficients for a horizontal circular cross section heaving below a free surface; b) wave-damping coefficients.

When each model was oscillated in air over the frequency range for sway and heave to obtain tare force measurements, the amplitudes of the oscillator and models were identical. The measured inertia forces, compared to the ideal inertia forces $m\eta\omega^2$ and $m\zeta\omega^2$, became smaller as $\bar{\omega}$ decreased below 0.4, leveled off for the circular cross section, and increased very slightly for the square cross section, as $\bar{\omega}$ increased above 0.4. Deviations over the frequency range were within the measuring accuracy.

Measured signals coming from the force gages were processed automatically by the signal processor (described in Ref. 6) at the end of each test to get in-phase and quadrature force components that corresponded to the added mass and damping, respectively. Wave-damping force components were obtained by subtracting the damping components measured in simulated infinite water from the dampings measured at each submergence.

Simulation of Infinite Water

The damping force components, to produce no wave damping, were measured by swaying and heaving the models over the frequency range in simulated infinite water. Infinite depth was simulated by keeping the tank water depth at $\bar{h} = 33.8$. The \bar{h} is defined as $\bar{h} = h/a$, where h is the water depth. The infinite water was simulated at the submergence of

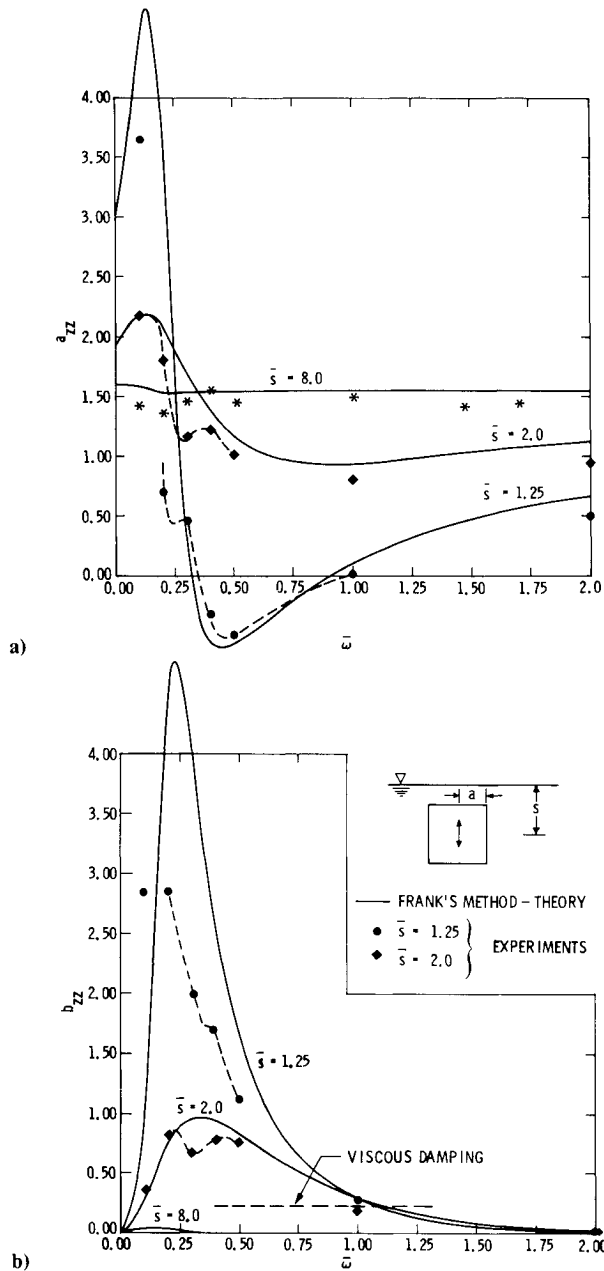


Fig. 4 a) Added-mass coefficients for a horizontal square cross section heaving below a free surface; b) wave-damping coefficients.

$\bar{s} = 8$, for which negligible outgoing waves were produced. The \bar{s} is defined as $\bar{s} = s/a$, where s is the distance of the model axis below the still-water surface and a is the radius or half-beam of the model. The simulation at $\bar{s} > 8$ was difficult, because the supports joining the model to the PMM were not absolutely rigid when subjected to the forces produced by the large models during sway oscillations at $\bar{s} = 8$. The $\bar{s} = 8$ submergence came close to the simulation of infinite water, but a small free-surface effect still could be detected at the lower end of the frequency range in both the added-mass and damping coefficients (Figs. 3-6). However, the damping at $\bar{s} = 8$ leveled off at higher frequencies, at which negligible outgoing waves were produced and the wave damping was faired through the damping points in this high-frequency range and was assumed to be the damping for the model in infinite water.

Linearity

In order to establish linearity of the measured forces with the oscillation amplitudes, each model was oscillated separately for swaying and heaving at the beginning of testing

each model over the range of amplitudes and frequency at the shallowest submergence tested ($\bar{s} = 1.25$) (Fig. 2 and Table 1). Linear amplitudes in each mode of oscillation of each model were chosen over the frequency range, using the in-phase force curves as a function of oscillation amplitudes. A typical in-phase force-to-amplitude relationship for the circular cross section is presented in Fig. 2. Maximum linear amplitudes of oscillation decreased slightly as the frequency decreased. In the lower end of the frequency range, the experimental points were scattered slightly because of smaller force amplitudes compared to the larger amplitudes at the higher frequency range. Thus the larger values among the oscillation amplitudes that assure the linearity over the frequency range were determined as $\zeta = 1.016$ cm for heaving of both cross sections, $\eta = 2.54$ cm for swaying of the circular cross section, and $\eta = 2.032$ cm for swaying of the square cross section (Table 1). These amplitudes, taken at $\bar{s} = 1.25$, were used to measure and analyze the forces at all model submergences, $\bar{s} \geq 1.25$.

Frequency and Submergence

The nondimensional oscillation frequency range selected for practical applications to many existing, floating drilling structures³ was $0.05 \leq \bar{\omega} \leq 2.0$. The wave period range of interest for ocean operations can be $5 \leq T \leq 25$ sec. For example, this wave period range corresponds to $0.035 < \bar{\omega} < 1.0$ for the horizontal, submerged structural members of Project MOHOLE drilling platform.³

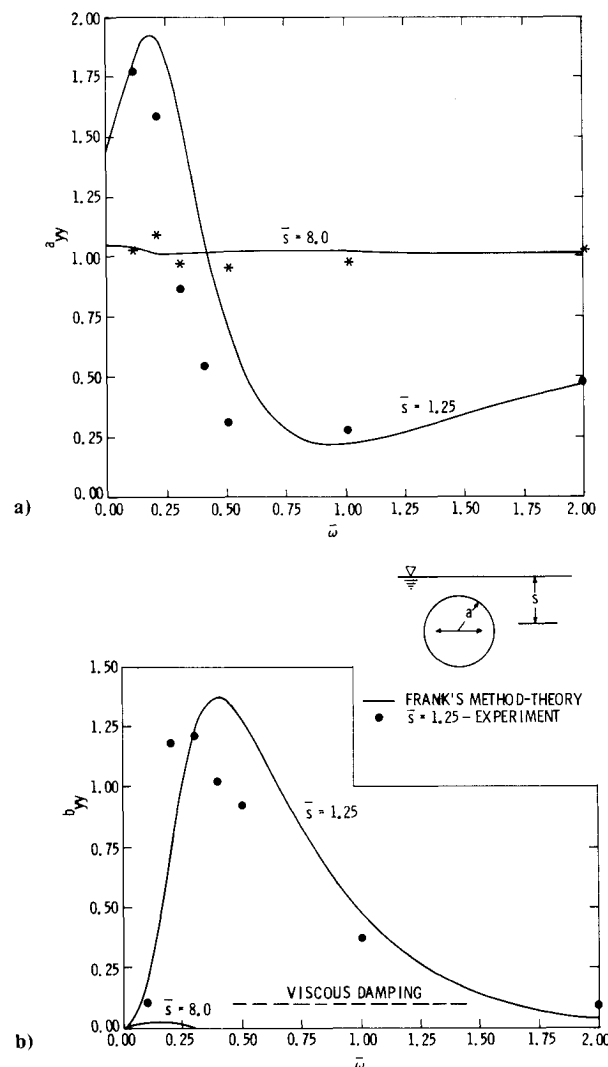


Fig. 5 a) Added-mass coefficients for a horizontal circular cross section swaying below a free surface; b) wave-damping coefficients.

Submergences of the model axis below the still-water surface were selected as $\bar{s} = 1.25, 1.6, 2.0$, and 8.0 , suitable for practical applications to many existing, floating drilling structures. For the MOHOLE platform,³ the drilling draft range corresponds to $2.43 \leq \bar{s} \leq 3.0$, and the survival draft corresponds to $\bar{s} = 1.57$. For sway of the circular-cross-section model, only $\bar{s} = 1.25$ was tested. The test series were programmed to emphasize the free-surface effect on the coefficients as a function of the model submergence and to check the validity limit of the theory² over practical ranges of frequency and submergence. Coefficients for $\bar{s} = 8$ were affected little by the free surface. Experiments for $8 > \bar{s} > 2$ were not carried out, since comparison of a few data points with theory for $\bar{s} = 3$ showed that the theoretical computations were accurate.

Force Coefficients

The nondimensional, added-mass coefficients a_{jj} and wave-damping coefficients b_{jj} are obtained after removing the in-air tares and the damping caused by viscosity:

$$a_{yy} = Y_i / m\omega^2 \eta - m' / m \quad \text{for sway } (j=2)$$

$$a_{zz} = Z_i / m\omega^2 \zeta - m' / m \quad \text{for heave } (j=3)$$

$$b_{yy} = Y_0 / m\omega \eta - b_{yy}^* / m \quad \text{for sway } (j=2)$$

$$b_{zz} = Z_0 / m\omega \zeta - b_{zz}^* / m \quad \text{for heave } (j=3)$$

IV. Discussion of Results

Direction of Oscillations (Heave and Sway)

Nondimensional added-mass and wave-damping coefficients are presented in Figs. 3 and 4 for heaving and in Figs. 5 and 6 for swaying. The experimental points have been derived directly from the measurements without smoothing a force coefficient curve through the measured points. The consistency of the experiments is satisfactory. Dip points (see the dotted lines) on the force coefficient curves at the frequency $\bar{\omega} \approx 0.3$ for heaving were measured repeatedly for both models and are discussed later.

Measurements for the circular cross section (Fig. 1) consistently showed that both the added mass and damping at $\bar{s} = 1.25$ are shifted slightly in frequencies between heaving and swaying. The agreement with theoretical computations² is better for heaving than for swaying. Theory predicts identical coefficient values for any direction of oscillation of the circular cross section but does not agree very well with the experimental sway coefficients. Upon overlaying the coefficient curves and shifting the frequency between the heave and sway curves, the curves appear to become nearly identical.

For the square cross section, both the measurements and theoretical computations show that peak coefficient values are larger for heaving than for swaying. Comparisons of the measured coefficients with the theoretical values show that the agreement is reasonably good, except at $\bar{\omega} < 0.5$ and $\bar{s} = 1.25$, and is better for heaving than for swaying. For swaying at $\bar{s} \leq 2.0$ and $\bar{\omega} < 0.5$, the experimental points are at larger values than the theoretical points. For heaving at $\bar{s} = 1.25$ and $\bar{\omega} < 0.5$, the experimental points are at smaller values than the theoretical points.

Submergence and Oscillation Frequency

For infinite fluid, the added-mass coefficients are constants⁵ and are independent of the oscillation frequencies for small amplitudes; the corresponding wave-damping coefficients are zero. For a fluid that is bounded by a free surface, the coefficients vary as a function of oscillation frequency and submergence of the models.

As the submergence of the model becomes shallower, the free-surface effect gets stronger and is more pronounced in the lower end of the frequency range at which the maximum and minimum values of added-mass coefficients are found. This lower end of the frequency range is of interest for

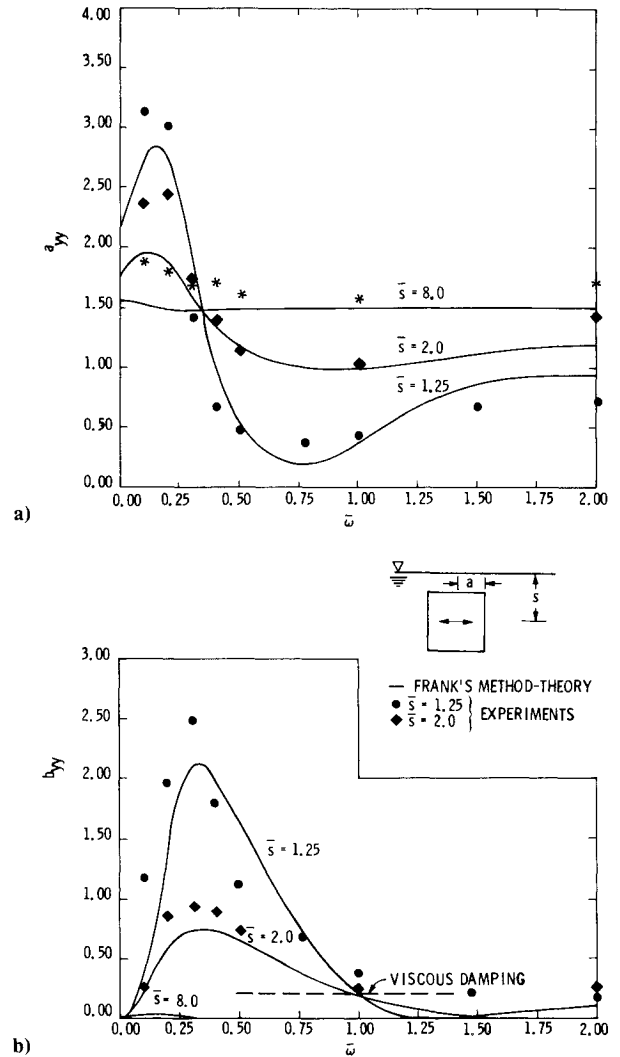


Fig. 6 a) Added-mass coefficients for a horizontal square cross section swaying below a free surface; b) wave-damping coefficients.

practical operations of floating ocean structures. Decrease in model submergence increases the maximum values of the added-mass and wave-damping coefficients and also reduces the minimum values of the added-mass coefficients. For square-cross-section heaving very close to the free surface ($\bar{s} = 1.25$), the experiments and theoretical computations² both show that the minimum value of the added-mass coefficients becomes negative, to which much attention was paid during testing. The negative experimental points were measured repeatedly. This measurement of the negative added-mass coefficients can clear partly the concern of Yamamoto,¹ whose theoretical computations with $\bar{s} = 1.0$ for the circular cross section were thought to have been in error. For the same circular cross section at $1.0 \leq \bar{s} \leq 1.15$, computations by Frank's method also give negative values of added-mass coefficients over the same frequency range as that by Yamamoto; at these shallow submergences, theoretical computations may not be very accurate. For $\bar{s} = 1.0$, the absolute, maximum, and minimum values of added-mass coefficients computed by Frank's method are much larger than the corresponding values computed by Yamamoto.¹ Comparisons of the theoretical methods in Refs. 1 and 2 are not within the scope of this paper and are not discussed further.

At high frequencies, $\bar{\omega} \geq 2.0$, the added-mass coefficients of both models approach constants for the respective submergences, and the wave-damping coefficients of the circular-cross-section model approach zero. For sway of the square

cross section at the higher frequencies, the wave-damping coefficients become very small but appear to increase slightly with an increase of frequency, as the theoretical curve shows. For heave of the square cross section, wave-damping coefficients approach zero at high frequencies.

Generally the experimental coefficients agree well with the theoretical computations² for the submergences tested and increasingly improve with increased submergence. Small deviations in maximum values of the coefficients can be noticed at $\bar{\omega} < 0.5$ and $\bar{s} < 2$, the sway coefficients deviating more than the heave coefficients. Compared with the wave damping measured at $\bar{s} \leq 2$, damping when measured at $\bar{s} = 8$ is small, the comparison being nondimensionalized for both sway and heave by identical factors, and is assumed to be caused by the viscosity effect. Except for $\bar{s} = 8$, no tests where $\bar{s} > 2$ were carried out because the theoretical coefficients at $\bar{s} = 2$ and a few points at $\bar{s} = 3$ agreed well with the corresponding experimental points and because accuracy was expected to improve for predictions by the potential theory where the model oscillation was far from the free surface.

At $\bar{s} \geq 8$, the free-surface effect on the measured coefficients practically disappears and can be neglected for practical purposes. That is, the added-mass coefficients of bodies of various cross sections approach their respective constant values for infinite fluid, the corresponding wave damping being zero. For the circular-cross-section heaving at $\bar{s} = 8$ (Fig. 3), the experimental wave-damping coefficients measured were significantly larger than the theoretical computations; possible reasons for the deviation were not found. For the square cross section at $\bar{s} = 8$, the experimental wave-damping coefficients for heaving and swaying were only slightly larger than the theoretical computations. Previously, the damping coefficients measured at higher frequencies for $\bar{s} = 8$ had been assumed to be due to viscosity effect alone. Under identical normalization factors (Figs. 4 and 6), the measured viscous-damping coefficients were found to be smaller than the wave-damping coefficients of the models tested for submergences, $\bar{s} \leq 2$.

Discussion of Dips in the Heave Coefficient Curves

For shallow submergences of either model, the experiments consistently showed dips at $\bar{\omega} \approx 0.3$ on the coefficient curves of heave added mass and wave damping (Figs. 3 and 4). The dip points were measured at submergences of $\bar{s} \leq 2$ for the square

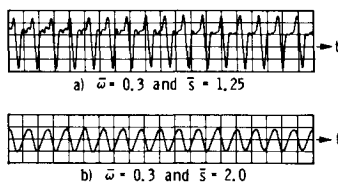


Fig. 7 Sample records of waves generated by a heaving circular-cross-section model: a) dip points on the coefficient curve were obtained at $\bar{\omega} = 0.3$ and $\bar{s} = 1.25$; b) no dip points on the coefficient curve were obtained at $\bar{\omega} = 0.3$ and $\bar{s} = 2.0$

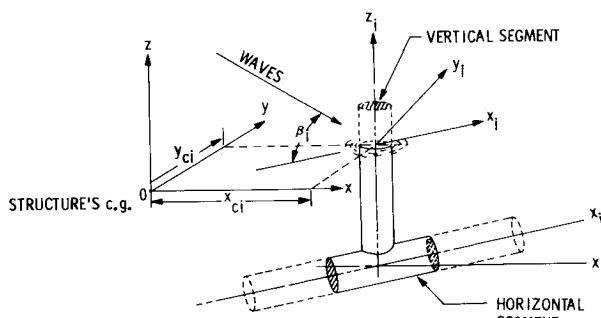


Fig. 8 Coordinate systems for a floating structure.

cross section and $\bar{s} \leq 1.6$ for the circular cross section. However, theoretical computations do not predict any dips regardless of submergence. For swaying, both theoretical computations and experimental results show no dips over the frequency range for all submergences. No clear reasons have been found for these dips appearing at $\bar{\omega} \approx 0.3$ for shallow submergences. Judged on the basis of time-history recordings of waves (Fig. 7) and visual observations of surface flows, the following speculation can be made as to the probable reasons for these dip points.

Nonsinusoidal waves (Fig. 7) were recorded in the lower frequencies for heave oscillations of the circular cross section at shallow submergences. Compared to sinusoidal waves of $\bar{\omega} \approx 0.3$ generated by heave at $\bar{s} = 2$, nonsinusoidal waves of the same frequency were generated at $\bar{\omega} \approx 0.3$ by the heave at $\bar{s} = 1.25$. For the latter submergence, the coefficient curve had a dip at $\bar{\omega} \approx 0.3$. The wave frequency was the same as the oscillation frequency of the PMM oscillator for all of the submergences tested. For nonsinusoidal waves, a higher-frequency component was superposed on the model frequency.

Also, visual observations of the surface flows on the heaving square cross section at $\bar{\omega} \leq 0.5$ and $\bar{s} = 1.25$ showed interferences of incoming flows of surface fluid over the top surface of the model. The flows incoming from both directions splashed above the top centerline of the model, that is, parallel to the model axis, at intervals equal to the oscillation frequency. Upon splashing, the surface flows joined the outgoing waves. The heave oscillation of the model during downstroking at $\bar{\omega} \leq 0.5$ at shallow submergences instantly created a depression on the surface of water above the model. This periodically depressed surface was filled instantly by incoming flows from both directions, causing surface splashes at the surface on the top centerline of the model. Upon splashing, the flows appeared to be reflected in the outgoing directions, thus generating the higher-frequency component in addition to the model frequency. The instants of splashing relative to the model oscillations were not recorded. Upstroking motion displaced water above the top surface of the model in the outgoing directions. High frequencies, $\bar{\omega} > 0.5$, did not allow enough time during one complete cycle of the model oscillation for surface water flows to fill the depressed surface completely or to splash. At $\bar{\omega} = 2$, it appeared that constant volumes of water above the square cross section oscillate with the heaving model, and that negligibly small outgoing waves were generated.

The splashing or interference of the flows above the heaving model incoming from opposing directions appeared to generate nonsinusoidal outgoing waves at $\bar{\omega} \approx 0.3$. The splashing must have accompanied downward flows acting on the model. It is speculated that these interferences may have exerted external forces implicitly created by and acting on the heaving model to cause the dip in the heave coefficient curve. It is noted that the potential theories^{1,2} do not take into account these interferences. For the sway oscillations, depressions of the water surface or flow interaction such as that observed for heaving were not observed.

V. Applications to Motions of Floating Structures

A Cartesian (x, y, z) coordinate system has its origin at the center of gravity (c.g.) of a floating structure with the undisturbed free surface at $(0, 0, 0)$ (Fig. 8). Structural members are idealized as being segments of continuous surfaces, vertical and horizontal. Hydrodynamically, each individual segment for the submerged portion of the structural members is treated independent of each other. Another Cartesian (x_i, y_i, z_i) coordinate system is introduced at the center of the i th segment volume and has its origin at a point $(x_{ci}, y_{ci}, 0)$.

Slopes of the incident waves are assumed to be small so that the waves may be described as infinitesimal. It is assumed that the oscillatory, rigid-body responses of the structure are linear

and harmonic. The six linear, coupled differential equations of motion can be written from Ref. 3:

$$\sum_{k=1}^6 [(M_{jk} + A_{jk}) \ddot{\chi}_k + B_{jk} \dot{\chi}_k + C_{jk} \chi_k] = F_j e^{i\omega t}$$

where $j = 1, 2, \dots, 6$. M_{jk} are the components of the generalized mass matrix for the structure, A_{jk} and B_{jk} are the added mass coefficients and damping coefficients, respectively, C_{jk} are the hydrostatic restoring coefficients, and F_j are the exciting forces and moments. The dots indicate time derivatives, $\partial/\partial t$ and $\partial^2/\partial t^2$, so that $\dot{\chi}_k$ and $\ddot{\chi}_k$ stand for the velocity and acceleration, respectively, of the structure's c.g. A_{jk} , B_{jk} , C_{jk} , and F_j ($j, k = 1, 2, \dots, 6$) can be expressed in terms of the segmental values in the (x_i, y_i, z_i) coordinates, a_{jk} , b_{jk} , c_{jk} , and f_j ($j, k = 1, 2, 3$) (see Ref. 3 for details).

The coefficients a_{jk} and b_{jk} are reported in this paper for the case of $j = k$, $j = 2, 3$. Use of such A_{jk} , B_{jk} , and F_j assumes that the possible hydrodynamic interference effects at the intersections of the vertical and horizontal members, or between the segments, are negligibly small.

VI. Conclusions and Recommendations

Comparisons of experimental added-mass and wave-damping coefficients with theoretical coefficients computed by Frank's method show good agreement for practical applications, agreements being better for heaving than for swaying. Also, the comparisons show better agreement for the circular cross section than for the square one. For the circular cross section, the measured coefficient curves show a slight shift in frequencies between heaving and swaying, and comparison of experimental points with theoretical computations² shows better agreement for heaving than for swaying. Frank's theory does not distinguish the direction of oscillation for the coefficients.

Agreement of the experimental coefficients with theoretical values is generally good for all submergences tested except for a few small deviations, and improves as the submergence increases. The few exceptions include small deviations in the maximum values of the coefficients at dimensionless frequencies $\bar{\omega} < 0.5$ and submergence $\bar{s} < 2$, these deviations being larger for sway coefficients than for heave coefficients. The deviations become smaller as the frequency and sub-

mergence increase. At the highest frequencies tested for the square cross section, the measured added-mass coefficients were slightly lower than the computed values. Compared to the wave damping measured for $\bar{s} < 2$, damping caused by the viscosity effect was small when nondimensionalized by the same factor. Based on the data for submergence of four times the model diameter or beam, it can be concluded for engineering applications that for $\bar{s} \geq 8$ the added-mass coefficients are constants, as would be obtained for infinite fluid, and wave damping is practically zero.

Dip points on the added-mass and wave-damping coefficients are believed to exist near the nondimensional frequency of 0.3 for models heaving near the free surface. This can not be predicted by the potential theories cited in this paper. The speculated reason in this paper for the existence of the dip points may be checked by measurements of waves and of pressure distributions around the model cross section, especially on the top surface of the models. Motion pictures of this flow interference relative to the model oscillations may aid such an analysis. It is noted that the present experimental setup and procedure apply to Ref. 3 for the oval footing with a vertical column of circular cross section.

References

- ¹Yamamoto, Y., "On the Oscillating Body under the Water Surface," *Journal of Zosen Kiokai*, Vol. 77, July 1955, pp. 29-41.
- ²Frank, W., "Oscillation of a Cylinder in or below the Free Surface of Deep Fluids," Naval Ship Research & Development Center, Navy Dept., Rept. 2357, 1967.
- ³Chung, J.S., "Motion of a Floating Structure in Water of Uniform Depth," *Journal of Hydraulics*, Vol. 10, July 1976, pp. 65-73.
- ⁴St. Denis, M., "On the Motion of Oceanic Platform," *International Symposium on the Dynamics of Marine Vehicles and Structures in Waves*, Inst. of Mechanical Engineers, London, April 1-5, 1974, pp. 121-142.
- ⁵Wendel, K., "Hydrodynamic Mass and Hydrodynamic Moments of Inertia," David Taylor Model Basin, Navy Dept., Transl. 260, 1956.
- ⁶Goodman, A., "Description and Operation of Planar Motion Mechanism System," *Hydraulics, Inc.*, Tech. Manual 754-1, April 1968.
- ⁷Morison, J.R., O'Brien, M.P., Johnson, J.W. and Schaaf, S.A., "The Force Exerted by Surface Waves on Piles," *Petroleum Transactions*, American Society of Mining Engineers, Vol. 189, 1950, pp. 149-157.